Correlation between the Steric Bulk of the Distal E7 and E11 Residues and the Tilt of the FeCN Unit in Cyanometmyoglobin As Determined by NMR from the Orientation of the Magnetic Axes in Single and Double Point Mutants†

Krishnakumar Rajarathnam,‡ Jun Qin,‡ Gerd N. La Mar,*,‡ Mark L. Chiu,§ and Stephen G. Sligar§

Department of Chemistry, University of California, Davis, California 95616, and Department of Chemistry, Biochemistry and Biophysics, University of Illinois, Urbana, Illinois 61801

Received November 10, 1993; Revised Manuscript Received March 9, 1994®

ABSTRACT: The amino acids in the heme pocket of sperm whale myoglobin single E11 and double E7 and E11 point mutants in the metcyano form have been assigned by NMR methods to assess the role of steric bulk in modulating ligand tilt. The five mutants investigated are the single mutants His64(E7)→Gly (H[E7]G), Val68(E11)→Ile (V[E11]I), and Val68(E11)→Ala (V[E11]A) and the double mutants His64-(E7)→Gly:Val68(E11)→Ile (H,V[E7,E11]G,I) and His64(E7)→Gly:Val68(E11)→Ala (H,V[E7,E11]G,A). The dipolar (NOESY) contacts on the proximal side of the heme confirm a conserved molecular structure for all of the mutants. The proximal residue coordinates, together with the dipolar shifts for proximal side residues, quantitatively yield the orientations of the magnetic susceptibility tensors, whose major axis corresponds to the orientation of the ligand. It is observed that upon reduction of the steric bulk in the V[E11]A mutant, the tilt of the ligand is significantly reduced (~8°) from that in the wild type (WT) (~16°), with little change in the direction of tilt. In the case of increased steric bulk at position 68 in the V[E11]I mutant, it is observed that the extent and direction of the tilt are essentially the same as in WT, and it is shown that this is due to the fact that Ile68 is oriented in the pocket with its $C_\delta H_3$ directed away from the iron. The removal of the bulky imidazole side chain in the H[E7]G and H[E7]V mutants leaves the extent of tilt unchanged from that in WT, but with a direction of tilt rotated by ~40° that has been interpreted in terms of the energy surface of the heme pocket [Rajarathnam, K., *et al.* (1993) *Biochemistry 32*, 5670–5680]. Hence, the E7 and E11 residues appear to control the direction and the extent of tilt of the bound ligand, respectively. In the double mutants, the influences of the E7 and E11 substitutions are essentially additive, with the ligand tilt adopting the direction of the H[E7]G single mutant and the extent of tilt of the V[E11]A or V[E11]I single mutant. The extent of the ligand tilt determined herein for the various cyanometmyoglobin mutants does not correlate with the kinetics or thermodynamics of CO ligation, indicating that factors other than steric effects, such as polarity of the heme pocket, play an important role in modulating ligand binding.

Myoglobins (Mbs[1]) as a class of proteins have been studied extensively and remain the paradigm for interaction between proteins and small ligands. A number of crystallographic and molecular dynamics studies have shown that most aspects of ligand binding are modulated by the highly conserved distal His(E7)[2] and Val(E11) residues (Case & Karplus, 1979; Phillips, 1980; Kuriyan *et al.*, 1986; Kottalam & Case, 1988; Elber & Karplus, 1990). Considerable importance has been devoted to the binding of O_2 and CO, because of their biological relevance. It is believed that Mbs and hemoglobins (Hbs) have evolved to selectively bind O_2 over CO, and this selectivity has been attributed to the ability of distal histidine to stabilize O_2 binding by H-bonding and destabilize CO binding by steric interactions (Phillips, 1980; Collman *et al.*, 1976). The steric destabilization of bound CO has been inferred from the observation that the ligand atoms for CO are well-displaced from the heme normal in Mbs and Hbs (Deatherage *et al.*, 1976; Steigemann & Weber, 1979; Kuriyan *et al.*, 1986; Derewenda *et al.*, 1990; Cheng & Schoenborn, 1991), while in model compounds the Fe–CO bond is both linear and perpendicular to the heme. Although recent kinetic studies of a number of single and double E7 and E11 mutants have indeed shown that these residues play a major role in affecting the observed kinetics, the molecular bases for the observed kinetics remain unclear (Egeberg *et al.*, 1990; Rohlfs *et al.*, 1990; Smerdon *et al.*, 1991; Balasubramanian *et al.*, 1993).

One aspect of ligand binding that is of considerable interest is the relationship between the nature and the extent of the tilt of the Fe–CO bond and the steric bulk at the distal E7 and E11 positions. High-resolution X-ray structures are capable of providing the necessary answers, and more recently,

† This research was supported by grants from the National Institutes of Health [HL 16087 (G.N.L.), GM 33775 (S.G.S.), and GM 31756 (S.G.S.)]. The Ω500 NMR instrument was purchased, in part, with funds provided by the National Institutes of Health (RR-04795) and the National Science Foundation (BBS-88-04739).

‡ University of California at Davis.

§ University of Illinois.

® Abstract published in *Advance ACS Abstracts,* April 15, 1994.

[1] Abbreviations: Mb, myoglobin; Hb, hemoglobin; metMbCN, cyanometmyoglobin; NMR, nuclear magnetic resonance; WEFT, water-eliminated Fourier transform; DSS, 2,2-dimethyl-2-silapentane-5-sulfonic acid; COSY, two-dimensional bond correlation spectroscopy; NOE, nuclear Overhauser effect; NOESY, two-dimensional nuclear Overhauser effect spectroscopy; V[E11]A, Val68→Ala mutation at position E11; V[E11]I, Val68→Ile mutation at position E11; H[E7]G, His64→Gly mutation at position E7; H,V[E7,E11]G,I, His64→Gly mutation at position E7 and Val68→Ile mutation at position E11; H,V[E7,E11]G,A, His64→Gly mutation at position E7 and Val68→Ala mutation at position E11.

[2] E7 and E11 are alphanumerical codes referring to the position of the residue in the wild-type sperm whale myoglobin sequence. E7 and E11 are the seventh and eleventh residues in the E helix, respectively (Dickerson & Geis, 1983).

0006-2960/94/0433-5493$04.50/0

^{1}H NMR has been shown to yield the same information for metMbCN in solution (Emerson & La Mar, 1990b; Rajarathnam *et al.*, 1992, 1993; Qin *et al.*, 1993a,b). The $Fe^{3+}CN$ and $Fe^{2+}CO$ units are expected to be isostructural, and in three cases where both forms have been studied, sperm whale Mb (Cheng & Schoenborn, 1991; Emerson & La Mar, 1990b), *Chironomus* monomeric Hb (Steigemann & Weber, 1979), and *Aplysia limacina* Mb (Qin *et al.*, 1993a; Conti *et al.*, 1993), the ligand tilts differ for the three proteins, but are very similar for the two ligands in a given protein. The ^{1}H NMR method relies on determining the chemical shifts of the strongly dipolar shifted protons of the amino acids in the heme pocket, from which the orientation of the magnetic axes is determined.

The major magnetic axis in a low-spin ferric heme is related to the tilt from the heme normal of the strongest ligand (cyanide), as discussed previously (Rajarathnam *et al.*, 1993). The correlation between major magnetic axis and ligand tilt is directly supported by observing essentially coincident ligation and magnetic vectors by X-ray and/or neutron diffraction and ^{1}H NMR in sperm whale metMbCN (Emerson & La Mar, 1990b; M. Bolognesi, personal communication), *Chironomus* metHbCN (Steigemann & Weber, 1979; W. Zhang, G. N. La Mar and K. Gersonde, unpublished results), *Aplysia limacina* metMbCN (Qin *et al.*, 1993a; Conti *et al.*, 1993), and ferricytochrome *c* (Feng *et al.*, 1990). Such magnetic axis determinations in the H[E7]G and H[E7]V metMbCN point mutants (Rajarathnam *et al.*, 1992, 1993) have shown that the extent of the FeCN tilt is essentially unchanged from that in WT, but that the direction of the tilt is significantly changed. This observation contradicts the belief that the distal histidine is responsible for the extent of the tilt. Hence, we had suggested that the major determinant of the extent of tilt could be the steric bulk of the E11 residue.

In order to elucidate the role of steric bulk at the E11 position in the ligand tilt, we report herein the ^{1}H NMR determination of the orientations of the magnetic susceptibility tensors in the sperm whale E11 Ala and Ile point mutants (V[E11]A and V[E11]I), possessing substitutions of reduced and increased steric bulk, respectively. We also pursue the assignment and magnetic axis determination in the two double mutants where E11 is again substituted by Ala or Ile, but with the additional substitution of Gly for His(E7) (H,V-[E7,E11]G,A and H,V[E7,E11]G,I). The two double mutants allow an assessment of the interplay of the substitutions in controlling ligand tilt. Moreover, the ^{1}H NMR data for the substituted Ile residue will elucidate the influence of the E7 residue in modulating the disposition of the E11 Ile relative to the heme.

MATERIALS AND METHODS

Sample Preparation. The sperm whale V[E11]A, V[E11]I, H,V[E7,E11]G,A, and H,V[E7,E11]G,I Mb mutants were expressed and purified as previously described (Springer & Sligar, 1987). Cyanometmyoglobin (metMbCN) samples were prepared by exchanging the protein with a solution containing 200 mM KCl and 20 mM KCN in ^2H_2O at pH 8.6 on an Amicon ultracentrifuge cell. The concentrations of V[E11]I and H,V[E7,E11]G,I metMbCN samples were ~3 mM, and the more limited V[E11]A and H,V[E7,E11]G,A metMbCN samples were only <1 mM.

^{1}H NMR Measurements. All ^{1}H NMR spectra were collected on a GE Ω 500 spectrometer. The WEFT (Gupta, 1976) pulse sequence was used to produce spectra that suppress the slowly relaxing diamagnetic envelope and enhance the intensity of broad, rapidly relaxed signals. Nonselective T_1's were determined for strongly relaxed protons via the inversion–recovery experiment. Steady-state NOEs were determined by the procedure described in detail previously (Emerson & La Mar, 1990a). The distance to the iron, R_{Fe-i} of a paramagnetically relaxed proton i was determined via

$$T_{1i}/T_{1j} = R_{Fe-i}^6/R_{Fe-j}^6 \quad (1)$$

where T_{1i} and T_{1j} are the relaxation times of protons i and j. The reference proton, j, is the His93(F8) $N_\delta H$ with T_{ij} = 30 ms and $R_{Fe-j} \sim 5.0$ Å. The steady-state NOE to a strongly relaxed proton i with T_{1i} is given by

$$\eta_{j-i} = \sigma_{ij}T_{1i} \quad (2)$$

which yields an estimate for the i–j interproton distance, r_{ij}, via

$$\sigma_{ij} = -0.1\gamma 2h^2\gamma^4 r_{ij}^{-6}\tau_c \quad (3)$$

where a correlation time, $\tau_c \sim 9$ ns, is assumed.

The magnitude COSY (Aue *et al.*, 1976), MCOSY (n-type), spectra were collected at various temperatures from 10 to 45 °C in ^2H_2O over a spectral window of 16 000 Hz using 1024 t_2 complex points; 128–512 scans were collected for each block with a total of 400–512 t_1 blocks. The repetition time was 350 ms, and the total acquisition time varied from 8 to 15 h. Phase-sensitive 2D NOE (NOESY) spectra (Jeener *et al.*, 1979) were collected at 30 and 40 °C in ^2H_2O over a spectral window of 25 000 Hz using 1024 complex points in the t_2 dimension; 128–512 scans were collected for each of 256 t_1 increments, with mixing times ranging from 20 to 50 ms. The repetition time was 350 ms, and the total acquisition time ranged from 8 to 15 h. Quadrature detection along the t_1 dimension was achieved as described by States *et al.* (1982). The residual ^1H_2O signal was saturated using a decoupler pulse in the relaxation delay time. All 1D data were processed on a SPARC station using GE Unix Ω software. All 2D data were processed on a Silicon Graphics workstation using the Felix program written by Dr. Dennis Hare. Processing parameters are given in figure legends.

Magnetic Axis Determination. The magnetic axes were determined as described in detail previously (Emerson & La Mar, 1990b; Rajarathnam *et al.*, 1992, 1993). Experimental dipolar shifts for the structurally conserved proximal side of the heme were used as input to search for the Euler rotation angles, $R(\alpha,\beta,\gamma)$, that transform the molecular pseudo-symmetry coordinates (x',y',z' or γ,θ',Ω' (Figure 1)) readily obtained from crystal coordinates into magnetic axes, x,y,z, by minimizing the following global error function:

$$F/n = \sum^n |\delta_{dip}(\text{obs}) - \delta_{dip}(\text{calc})F(\alpha,\beta,\gamma)|^2 \quad (4)$$

where

$$\delta_{dip}(\text{calc}) = -\frac{1}{3N}[\Delta\chi_{ax}(3\cos^2\theta' - 1)r^{-3} + {}^3/_2\Delta\chi_{rh}(\sin\theta'\cos 2\Omega')r^{-3}] \quad (5)$$

and

$$\delta_{dip}(\text{obs}) = \delta_{obs} - \delta_{dia} \quad (6)$$

$\Delta\chi_{ax}$ and $\Delta\chi_{rh}$ are axial and rhombic anisotropies, respectively, and δ_{obs} is the observed chemical shift referenced to DSS. δ_{dia}

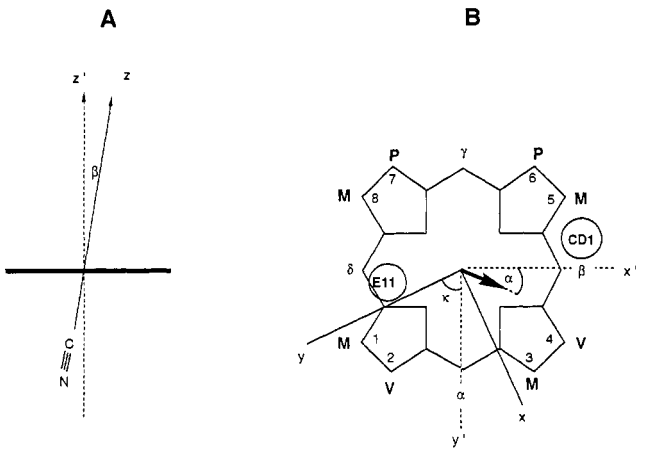

FIGURE 1: Orientation of the magnetic axes x, y, and z in the symmetry coordinates of the heme, x', y', z'. The FeCN is directed along the $-z$ direction. The Euler angles α, β, and γ represent (A) the tilt of the Fe–CN axis or z-axis from the heme normal (β), (B) the projection of the tilt on the heme plane (α), and the projection of the rhombic magnetic axes on the heme plane ($\kappa = \alpha + \gamma$).

is the shift in the isostructural diamagnetic MbCO complex (Dalvit & Wright, 1987; Theriault *et al.*, 1994), or it can be calculated for protons whose δ_{dia} values are not available by using the equation (Qin *et al.*, 1993a)

$$\delta_{dia} = \delta_{sec} + \delta_{rc} \quad (7)$$

where δ_{sec} is the shift of an amino acid proton typical for its secondary structural element (Wishart *et al.*, 1991), and δ_{rc} is the heme-induced ring current shift of the proton based on the WT coordinates using the eight loop model (Cross & Wright, 1985). Minimization of the error function F/n in eq 4 was performed over three parameters, α, β, and γ, using available $\Delta\chi_{ax}$ and $\Delta\chi_{rh}$ values or extended to all five parameters to yield both the Euler angles and anisotropies, as described in detail previously (Rajarathnam *et al.*, 1992).

Dipolar Shift Simulations. The dipolar shifts of the residues expected to be perturbed in the point mutant relative to WT (*i.e.*, distal side) and the substituted E11 residue were analyzed to assess the nature of the perturbations. In each case, both δ_{dia} and δ_{dip}(calc) were calculated on the basis of the proposed proton coordinates, using eqs 6 and 7, respectively (Rajarathnam *et al.*, 1993; Qin *et al.*, 1993a). The molecular modeling was carried out on a Silicon Graphics personal Iris for the MbCO structure using the MIDAS program.

RESULTS

Resonance Assignments. The resolved portions of the 500-MHz ^{1}H NMR spectra in ^1H_2O at 30 °C and pH 8.6 of WT, V[E11]I, V[E11]A, H[E7]G, H,V[E7,E11]G,I, and H,V-[E7,E11]G,A metMbCN are illustrated in Figure 2A–F, respectively. The spectra and the assignments for WT and H[E7]G metMbCN have been discussed in detail previously (Emerson & La Mar, 1990a; Rajarathnam *et al.*, 1992). The vertical lines connect the assigned resolved signals for several residues of interest, which shows that the chemical shifts of conserved resolved resonances are significantly affected by the substitution(s). The assignment strategy, outlined in detail for WT and several point mutants (Emerson & La Mar, 1990a; Rajarathnam *et al.*, 1992, 1993; Qin et al., 1993b), locates all resonances for the heme, the proximal residue side chains of Leu89(F4), Ala90(F5), His97(FG3), Ile99(FG5), Phe138-(H15), and His93(F8), the distal residue side chains of Phe43-(CD1), Thr67(E10), and Ala71(E14), and lastly, the sub-

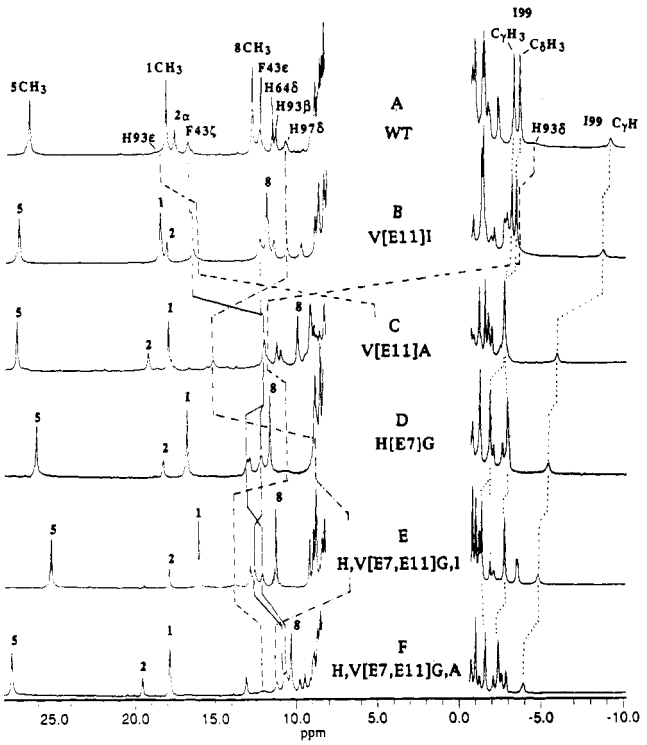

FIGURE 2: 500-MHz ^{1}H NMR spectra of the sperm whale metMbCN complex in ^2H_2O at pH 8.7 and 30 °C for (A) WT, (B) V[E11]I, (C) V[E11]A, (D) H[E7]G, (E) H,V[E7,E11]G,I, and (F) H,V-[E7,E11]G,A. The resolved heme methyls are labeled by the number of their position. The spectra of WT and H[E7]G metMbCN have been reported in detail previously (Emerson & La Mar, 1990a; Rajarathnam *et al.*, 1992). The assignments of resolved resonances of interest are given for WT metMbCN, and the positions of these resonances in the five mutants are indicated by vertical dashed (His93-(F8)), solid (Phe43(CD1)), dotted (Ile99(FG5)), and dot-dashed (His97(FG3)) lines.

stituted residues Ile68(E11) and Ala68(E11) (Table 1). The identification of the individual spin systems via bond correlation and their spatial placement relative to each other and with respect to the heme via dipolar correlation demonstrate that the structure of the proximal side in all four mutants is essentially very similar and that of the distal side is only slightly perturbed with respect to WT (Emerson & La Mar, 1990a; Yu *et al.*, 1990; Rajarathnam *et al.*, 1992). The chemical shift changes for noncoordinated residues among the different proteins, therefore, reflect changes in the orientations of the magnetic axes (see below). Representative COSY and NOESY data for H,V[E7,E11]G,I metMbCN are shown in Figure 3; additional relevant NMR data for V[E11]A, V[E11]I, and H,V[E7,E11]V,A metMbCN are provided in the supplementary material.

The conserved proximal and distal residues in the four mutants of interest exhibit (not shown; see the supplementary material) the same intraresidue COSY and intra- and interresidue NOESY cross peaks that were observed previously in WT and H[E7]G metMbCN (Emerson & La Mar, 1990a; Rajarathnam et al., 1992). The upfield region of the COSY spectrum (Figure 3A) for H,V[E7,E11]G,I exhibits the cross peaks of a complete Ile, whose $C_\alpha H$ exhibits a relatively strong NOESY cross peak to 1-CH_3 and a weak cross peak to 8-CH_3 (Figure 3C), identifying it as Ile68(E11). The only clearly resolved resonance is $C_\gamma H$ with $T_1 \sim 16$ ms ($R_{Fe} \sim 4.1$ Å). Saturation of this peak yields a *ca.* –5% NOE to the heme 1-CH_3 (not shown), which leads to a distance of ~3.5 Å using eq 2. Prominent intraresidue dipolar contacts for Ile68(E11) are the relatively strong cross peaks from $C_\gamma H$ to both $C_\gamma H_3$

Table 1: ^{1}H NMR Spectral Parameters for the Heme Pocket Amino Acids in WT, Single E7 or E11 Mutants, and E7/E11 Double Mutant metMbCN Complexes[a]

position	residue	peak	WT	V[E11]I	V[E11]A	H[E7]G	H,V[E7,E11]G,I	H,V[E7,E11]G,A
43(CD1)	Phe	$C_\delta H$'s	8.65	8.74	7.48	8.57	8.88	7.99
		$C_\epsilon H$'s	12.39	12.34	9.15	12.26	12.64	10.58
		$C_\zeta H$'s	16.93 (20)	16.48 (20)	12.0 (~20)	13.12 (~20)	12.14	10.71
64(E7)	Gly	$C_\alpha H$				5.83	*b*	5.59
		$C_\alpha H'$				6.33	*b*	6.46
	His	$C_\delta H$	11.57	11.82	11.26			
67(E10)	Thr	$C_\alpha H$	2.50	*b*	*b*	3.05	3.17	*b*
		$C_\beta H$	2.68	2.96	3.00	4.71	5.19	4.33
		$C_\gamma H_3$	−1.49 (280)	−1.44 (290)	−1.19	−1.23	−0.82	−1.05
68(E11)	Ala	$C_\alpha H$			−0.72 (~100)			−0.78[d]
		$C_\beta H_3$			2.32			*b*
	Val	$C_\alpha H$	−2.36 (110)			−0.26		
		$C_\beta H$	1.44			5.28		
		$C_{\gamma 1} H_3$	−0.97			1.27		
		$C_{\gamma 2} H_3$	−0.81			1.79		
	Ile	$C_\alpha H$		−0.83 (~140)			−0.42	
		$C_\beta H$		−1.92 (70)			3.47	
		$C_\gamma H$		1.27			−2.11 (16)	
		$C_\gamma H'$		0.97			3.28	
		$C_\gamma H_3$		−2.92 (35)			0.02	
		$C_\delta H_3$		3.70			3.08	
71(E14)	Ala	$C_\alpha H$	3.48	3.59	3.49	3.49	3.53	3.52
		$C_\beta H_3$	−0.09	−0.04	−0.24	−0.28	−0.16	−0.20
89(F4)	Leu	$C_\alpha H$	8.53	8.36	7.36	7.36	7.07	6.85
		$C_\beta H$	4.44	4.41	3.25	4.10	4.22	2.79
		$C_\beta H'$	3.82	3.80	2.69	3.33	3.28	3.50
		$C_\gamma H$	5.87	5.78	*c*	5.16	5.29	*c*
		$C_{\delta 1} H_3$	3.93	3.59	*c*	3.15	3.51	*c*
		$C_{\delta 2} H_3$	3.25	3.34	*c*	2.69	2.92	*c*
90(F5)	Ala	$C_\alpha H$	6.40	6.41	6.04	6.64	6.74	6.41
		$C_\beta H_3$	2.63	2.65	2.42	2.73	2.75	2.60
93(F8)	His	$C_\alpha H$	7.43	7.53	9.20	8.09	7.59	8.81
		$C_\beta H$	11.40	11.48	12.04	12.88	12.9	13.06
		$C_\beta H'$	6.34	6.49	7.22	8.80	9.24	8.94
		$C_\delta H$	−4.3	−3.6	~12.0	10.9	13.86	12.04
		$C_\epsilon H$	18.8	~16.5	*c*	*c*	*c*	*c*
97(FG3)	His	$C_\delta H$	10.79 (20)	10.63 (21)	15.22 (19)	8.82	6.56	11.17 (20)
		$C_\epsilon H$	6.84	6.83	7.66	6.17	5.77	6.61
99(FG5)	Ile	$C_\alpha H$	2.38	2.58	2.96	3.14	3.21	2.98
		$C_\beta H$	−0.09	0.09	0.95	1.91	2.29	2.24
		$C_\gamma H$	−9.23 (67)	−8.73 (68)	−5.96 (70)	−5.36 (57)	−4.81 (70)	−3.96 (70)
		$C_\gamma H'$	−1.78	−1.58	0.34	0.06	0.09	1.01
		$C_\gamma H_3$	−3.34	−3.20	−2.73	−1.83	−1.36	−1.63
		$C_\delta H_3$	−3.70	−3.48	−2.76	−2.90	−2.77	−2.44
138(H15)	Phe	$C_\delta H_s$	7.02	7.01	6.29	7.10	7.44	7.00
		$C_\epsilon H_s$	6.94	7.11	6.59	7.22	7.58	7.16
		$C_\zeta H$	7.05	7.25	6.82	7.55	8.03	7.26

[a] Chemical shifts, in ppm, from DSS at 30 °C and pH ~8.7 and T_1, in ms, with uncertainty ±10% in parentheses. [b] Not observed or assigned. [c] Chemical shifts are not observed in the rapid repetition rate experiments and hence resonate under the diamagnetic envelope 5 ± 4 ppm. [d] Assignment should be considered as tentative.

and $C_\alpha H$, while $C_\gamma H'$ exhibits much weaker cross peaks (Figure 3B). The upfield COSY and NOESY spectra (not shown; see the supplementary material) for V[E11]I exhibit three hyperfine-shifted and relaxed signals not present in WT metMbCN that must arise from Ile68(E11), as confirmed by the characteristic $C_\alpha H$ NOE to 8-CH_3 and 1-CH_3 (Rajarathnam *et al.*, 1993). The Ile $C_\gamma H_3$ also exhibits a weak NOESY peak to the heme 8-CH_3. Intraresidue NOESY cross peaks of interest for Ile68(E11) are the intense $C_\alpha H$–$C_\beta H$, $C_\gamma H_3$–$C_\delta H_3$, and $C_\gamma H_3$–$C_\gamma H$ NOESY cross peaks (see the supplementary material). Two of the resolved Ile68(E11) signals, $C_\beta H$ and $C_\gamma H_3$, exhibit significant paramagnetic relaxation effects: $T_1 \sim 70$ ms ($R_{Fe} \sim 5.5$Å) and $T_1 \sim 35$ ms ($R_{Fe} \sim 4.9$Å), respectively. The chemical shifts and T_1 values for resolved resonances are listed in Table 1.

The lateral position of the E helix relative to the heme in the various mutants is conveniently monitored[3] by the ratio of steady-state NOEs between heme 1-CH_3 and 8-CH_3 and immobile E11 $C_\alpha H$ and E14 $C_\beta H_3$ (Rajarathnam *et al.*, 1993), defined as

$$Q(i) = \eta(1\text{-}CH_3 \rightarrow i)/\eta(8\text{-}CH_3 \rightarrow i) = r^{-6}(1\text{-}CH_3\text{–}i)/r^{-6}(8\text{-}CH_3\text{–}i) \quad (8)$$

where i is either E11 $C_\alpha H$ or E14 $C_\beta H_3$. In WT the ratios are Q(E11 $C_\alpha H$) ~ 0.8 and Q(E14 $C_\beta H_3$) ~ 0.52, which are consistent with the crystal structure (Rajarathnam *et al.*, 1993). These values for the mutant metMbCN complexes of interest are V[E11]I, Q(E11 $C_\alpha H$) ~ 0.5, Q(E14 $C_\beta H_3$) = 0.46; H,V[E7,E11]G,I, Q(E11 $C_\alpha H$) = 2.2, Q(E14 $C_\beta H_3$) = 0.77; V[E11]A, Q(E11 $C_\alpha H$) = 0.3, Q(E14 $C_\beta H_3$) = 0.4. Spectral congestion for V[E11]A allowed only a tentative assignment for Ala68 $C_\alpha H$ at −0.78 ppm.

Magnetic Axis Determination. The orientations of the magnetic axes were obtained from the three-parameter searches based on 9 and 14 data point input sets[4] (I), which

[3] Since steady-state NOE, $\eta(i \rightarrow j) = \sigma_{ij} T_{1j}$, comparison of two NOEs to the same proton j eliminates the dependence of T_{1j}, *i.e.*, $\eta(i \rightarrow j)/\eta(k \rightarrow j) = \sigma_{ij}/\sigma_{kj} = r_{kj}^6/r_{ij}^6$.

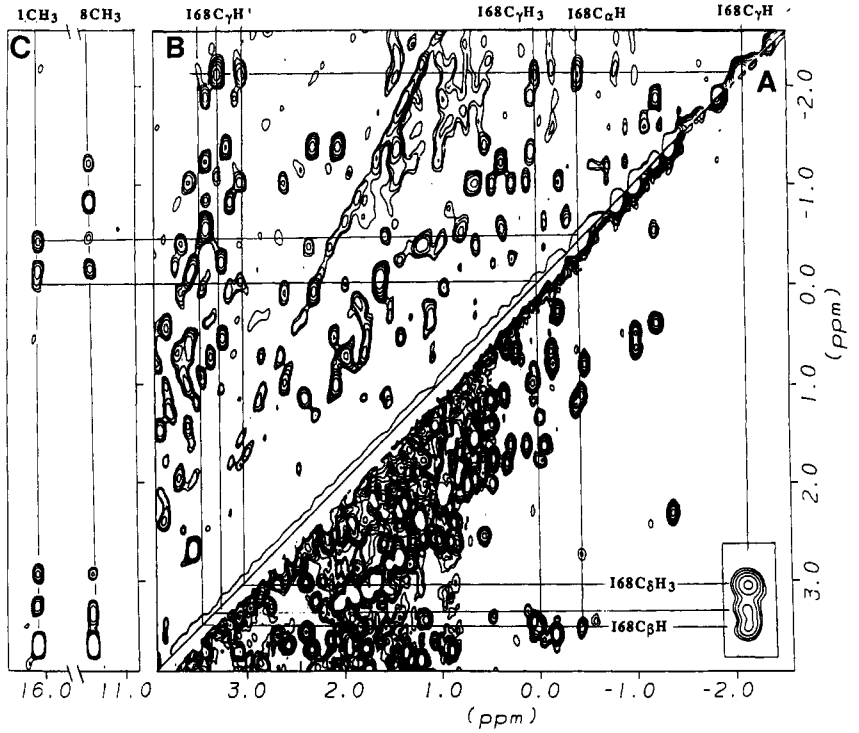

FIGURE 3: Split diagonal high-field portion of the (A) MCOSY and (B) NOESY spectra (mixing time, 20 ms) for H,V[E7,E11]G,I mutant metMbCN in ^2H_2O at pH 8.7 at 30 °C, illustrating the spin connectivity of the substituted Ile68(E11) residue and its intraresidue dipolar contacts. The low-field portion of the NOESY spectra (C) shows the Ile68(E11) to heme 1-CH_3 and 8-CH_3 dipolar contacts. The data were processed with 0°-shifted (MCOSY) and 30°-shifted (NOESY) sine-bell-squared window functions over 512 t_1 blocks and 512 t_2 points (MCOSY) or 512 t_1 blocks and 256 t_2 points (NOESY), prior to zero-filling to 2048 × 2048 points and Fourier transformation. Cross peaks in square boxes are obtained by application of the same window functions over only 256 t_1 × 256 t_2 points.

Table 2: Orientation of Magnetic Axes in WT and E7,E11 Mutant metMbCN

protein	Euler angles[a] α (deg)	β (deg)	κ = (α + γ) (deg)	$\overline{F/n}$[b]
WT[c]	9	16.0	38	0.038
V[E11]I	4	15.5	40	0.037
V[E11]A	30	8.5	41	0.058
H[E7]G[c]	−35	13.5	42	0.029
H[E7]V[d]	−34	14.5	39	0.040
H,V[E7,E11]G,I	−43	17.0	48	0.046
H,V[E7,E11]G,A	−38	9.0	40	0.024

[a] The maximum variations in the angles for the two different input data sets or between three- and five-parameter searches are 0.5° in β, 2° in α, and 3° in κ; for details of the individual searches, see the supplementary material. [b] The mean residual error function, in ppm², for the two three-parameter and one five-parameter least-squares fit to eq 4. [c] Data for the same input data sets were taken from Rajarathnam *et al.* (1992). [d] Data for the same input data sets were taken from Rajarathnam *et al.* (1993).

were previously shown to accurately define the orientation using the WT magnetic anisotropies, $\Delta\chi_{ax} = 1.10 \times 10^{-33}$ m^{-3} and $\Delta\chi_{rh} = 0.37 \times 10^{-33}$ m^{-3} (Rajarathnam *et al.*, 1992, 1993). A five-parameter search that also determined the anisotropies on the basis of the 14 data point input set yields Euler angles for each mutant that are remarkably invariant for the three separate searches, as found earlier for WT, H[E7]G, and H[E7]V (Rajarathnam *et al.*, 1992, 1993). The angles and mean error function for the four mutants of interest are listed in Table 2, where we also include the data for the three identical searches for WT, H[E7]G, and H[E7]V metMbCN reported previously. The ranges in the three angles for different determinations are 1°, 0.5°, and 2° for α, β, and κ (κ ~ α + γ), respectively. The details of the magnetic axes for the four mutants are listed in the supplementary material. The residual mean error functions for the three determinations (F/n) are as low as that observed for WT, where the determination of Euler angles was carried out for a number of input data sets varying from 5 to 37 input dipolar shifts (Rajarathnam *et al.*, 1992). Plots of δ_{dip}(calc) *vs* δ_{dip}(obs) fall on a straight line with a unit slope to the same degree as reported previously for WT (not shown). Moreover, the inclusion of anisotropies in the least-squares search leads to insignificant changes in the anisotropies, error functions, and Euler angles, indicating that the anisotropies of the mutants are conserved.

Orientation of Ile68 in E11 Mutants. The orientation of the substituted Ile in the single and double mutants can be semiquantitatively ascertained from a combination of constraints imposed by the distance to the iron (from T_1's), the intraresidue NOESY, and the Ile–heme NOESY cross-peak intensities. That the orientation is reasonable is supported by the calculation of the Ile dipolar shifts using the magnetic axes defined above. In WT MbCO, the H_α–C_α–C_β–H_β dihedral[5] angle φ of Val(E11) is 180°, and R_{Fe} ~ 6.7, 5.5, and 4.6 for the $C_\beta H$, $C_{\gamma 2}H_3$, and $C_{\gamma 1}H_3$, respectively (Kuriyan *et al.*, 1986); R_{Fe} for $C_{\gamma 1}H_3$ is consistent (eq 1) with $T_1(C_{\gamma 1}H_3)$ ~ 30 ± 10 ms in WT. Also, the Val $C_{\gamma 2}H_3$ exhibits a NOESY cross peak to 1-CH_3 in WT, as predicted by the 4-Å separation seen in the X-ray structure. Replacement of Val(E11) by Ile for an unaltered α–β bond leads to a conserved $C_{\gamma 2}H_3$-

[4] The sets of proximal side resonances were defined as D′ (14 peaks; all six Ile(FG5) signals, His(FG3) $C_\delta H$ and $C_\epsilon H$, Ala(F5) $C_\alpha H$ and $C_\beta H_3$, Leu(F4) $C_\alpha H$, and Phe(H15) ring protons) and E (9 peaks; all six Ile(FG5) signals, His(FG3), $C_\epsilon H$ and $C_\delta H$, and Leu(F4) $C_\alpha H$) in Rajarathnam *et al.* (1992).

[5] WT E11 Val was replaced by Ile using the MIDAS program from the University of California at San Francisco. The HC_α–$C_\beta H$ dihedral angle is defined as φ, with φ = 0 for the eclipsed configuration. Clockwise rotation is defined as increasing φ.

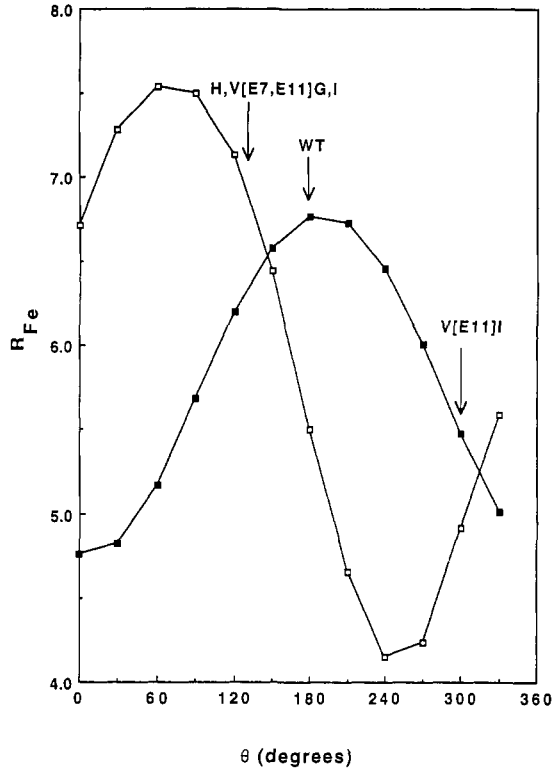

FIGURE 4: Plot of distances from the iron, R_{Fe}, of the Ile68(E11) $C_\beta H$ (■) and $C_\gamma H_3$ (□), as uniquely influenced by the bond rotation, ϕ. The fits between experimental relaxation data and R_{Fe} for the proteins of interest are shown by vertical arrows.

(Val)→$C_\gamma H_3$(Ile) and substitutes $C_{\gamma 1}H_3$(Val)→$C_\gamma H_2$–$C_\delta H_3$(Ile).

Ile68(E11) in the H,V[E7,E11]G,I metMbCN double mutant exhibits only a single resolved peak ($C_\gamma H$), and the side-chain orientation is determined initially from the relaxation and NOE restraints of this proton. The measured T_1 of 16 ms indicates that this proton is only 4.5 Å from the Fe. The $C_\gamma H$ gives an NOE to the heme 1-CH_3, and the intensity of the NOE (*ca.* –5%) indicates a distance of 4.1 Å between these protons (eqs 2 and 3). For the same dihedral angle as in the WT, $\phi \sim 180°$, it is observed that the distance constraint to the Fe is satisfied, but the distance between the $C_\gamma H$ and the heme 1-CH_3 is found to be 5.5 Å. However, a small counterclockwise rotation of the C_α–C_β bond by ~45° to $\phi \sim 135°$ satisfies both the relaxation and the heme–Ile NOE constraints. In addition to the $C_\gamma H$, fast repetition experiments (not shown) also indicate that both $C_\gamma H'$ and $C_\delta H_3$, which resonate in the diamagnetic region, have relatively short T_1's (~100 ms) and, hence, are in the vicinity of the Fe. This orientation of Ile68(E11) is consistent with the error function calculations for the dipolar shifts of the $C_\beta H$ and $C_\gamma H_3$ (broad minimum at $\phi \sim 90°$; not shown) and also with the relatively strong $C_\alpha H$–$C_\beta H$ COSY peak (Figure 3A) and the relative intensities of the Ile intraresidue cross peaks (Figure 3B). A weak $C_\gamma H_3$–$C_\delta H_3$ (Figure 3B) NOESY cross peak indicates a C_α–C_β–$C_{\gamma 1}$–C_δ angle of *ca.* –60°. The deduced Ile orientation in the H,V[E7,E11]G,I mutant places the ethyl group clearly toward the heme, whereas in the V[E11]I mutant, the ethyl group is pointed away from the heme (Figure 5B).

In the case of the V[E11]I mutant, Ile68(E11) exhibits two resolved signals that are significantly relaxed by the iron. The T_1 values of ~35 and 70 ms for the $C_\gamma H_3$ and $C_\beta H$, respectively, indicate distances to the iron (R_{Fe}) of ~4.9 and 5.6 Å, respectively. Figure 4 illustrates the effect of rotation[5] about the α–β bond on the R_{Fe} values for $C_\beta H$ and $C_\gamma H_3$. It

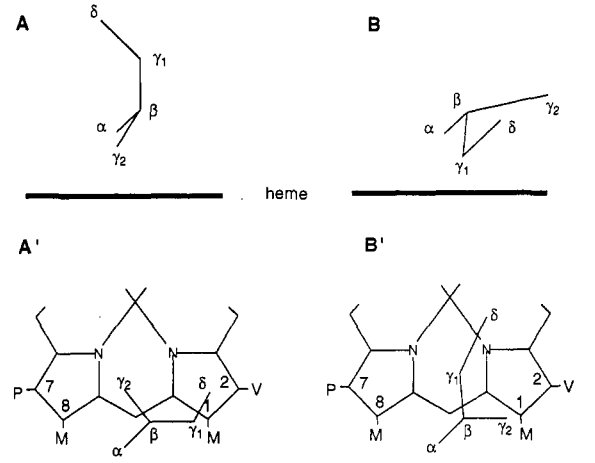

FIGURE 5: Schematic representation of the Ile(E11) orientation, heme face-on and heme edge-on, as viewed from the β-meso position for (A) V[E11]I and (B) H,V[E7,E11]G,I. The rotations for Ile68 in V[E11]I and H,V[E7,E11]G,I are clockwise and counterclockwise, respectively, from that of Val68 in WT.

is observed that only near $\phi \sim 300°$ (*i.e.*, a net ~120° clockwise rotation of the residue compared to Val(E11) in WT) are the predicted distances in good agreement with those obtained from the relaxation data. This rotational position is also supported by the calculation of the error function (a broad minimum $\phi \sim 300°$; not shown) and the NOE constraints. The loss of the NOESY cross peak to 1-CH_3 for $C_\gamma H_3$ of Ile (observed for $C_{\gamma 2}H_3$ of Val68 in WT) and the presence of a NOESY cross peak to 8-CH_3 (see the supplementary material) result from a decrease in the $C_\gamma H_3$ distance to 8-CH_3 by 1 Å and an increase in the distance to 1-CH_3 by 1 Å. The change in ϕ from 180° for Val68(E11) in WT to ~300° in the Ile68(E11) mutant is also supported by a relatively weak $C_\alpha H$–$C_\beta H$ COSY peak (supplementary material). Detailed analysis of the intensities of the Ile intraresidue cross peaks is consistent with the $C_\gamma H_3$ pointed toward the Fe and the $C_\delta H_3$ pointed away from the Fe, as shown in Figure 5A. Clearly, Ile68(E11) adopts an orientation in V[E11]I metMbCN with the increased bulk ($C_\delta H_3$) oriented well away from the binding site.

DISCUSSION

Orientation of Magnetic Axes. The observed chemical shifts for the proximal side amino acid residues show large changes due to mutations at the E7 and/or E11 positions, but exhibit essentially the same inter-amino acid and heme–amino acid dipolar contacts as in the WT (Emerson & La Mar, 1990a; Rajarathnam *et al.*, 1992). The shift changes are shown to arise solely due to changes in the orientations of the magnetic axes. The quality of the fits of the proximal side dipolar shift to eq 4, moreover, as reflected in the residual error functions (F/n) in Table 2, is as good as for WT and dictates that the proximal side structure is essentially conserved (Rajarathnam *et al.*, 1992). A strongly conserved proximal side structure for different ligation states that perturbs the distal pocket has been observed in the X-ray structures for *Aplysia limacina* Mb (Bolognesi *et al.*, 1989, 1990; Mattevi *et al.*, 1991; Conti *et al.*, 1993) and in different distal mutants of SW and porcine Mb (Smerdon *et al.*, 1991; Carver *et al.*, 1992). Extensive analysis of the influence of the nature of the NMR input data, the origin of the crystal coordinates, and the diamagnetic chemical shifts (Emerson & La Mar, 1991b; Rajarathnam *et al.*, 1992; Qin *et al.*, 1993a) has shown that the ^1H NMR method yields orientations for the magnetic axes reliable to

ranges of 1° in β (tilt of the major axis), 10° in α (direction of tilt of major axis), and 10° in κ (orientation of the rhombic axes), as defined in Figure 1. The variations in the angles observed for the three different searches made in this study are smaller, but the broader range of uncertainties is taken as a measure of the accuracy of the orientations.

The only conserved properties of the magnetic susceptibility tensor among the different E7 and E11 single and double mutant metMbCN proteins are the magnitudes of the magnetic anisotropies and the locations of the rhombic axes (Rajarathnam *et al.*, 1992, 1993; Qin *et al.*, 1993b). The conserved anisotropies are consistent with the observation of only minor variations of the *g* value in the low-temperature EPR spectra for a number of metMbCN mutants (Chiu, 1992). The essentially unchanged location of the rhombic axis, $\kappa \sim 40 \pm 10°$, is also confirmed by the very similar patterns of the heme methyl contact shift, both of which reflect the nature of the orbital hole (Shulman *et al.*, 1972). The orbital ground state has been proposed to be determined by the orientation of the imidazole plane of the axial His93(F8) relative to the heme, and the observed $\kappa \sim 40°$ is consistent with this proposal.

Extent/Direction of Ligand Tilt. Determination of the magnetic axes for the WT has shown that the tilt, $\beta \sim 16°$, and the direction of the tilt, $\alpha \sim 10°$, of the major magnetic axis are in good agreement with the tilt observed for the Fe–C vector of CO in both the X-ray (Kuriyan *et al.*, 1986) and the neutron diffraction (Cheng & Schoenborn, 1991) structures. We had recently shown from the NMR analysis (Rajarathnam *et al.*, 1992, 1993) that the extent of the major magnetic axis, and hence ligand tilt, in both H[E7]G and H[E7]V mutants ($\beta \sim 14°$) is similar to that of WT but is tilted in a different direction (rotated toward the γ-meso-H by $\sim$40°). The altered direction and conserved magnitude of the tilt were shown to be qualitatively consistent with earlier computations of the potential energy surface for CO in MbCO with and without the E7 in the distal pocket (Kuriyan *et al.*, 1986). From these studies, we had proposed that the steric bulk at the E7 position primarily affects the direction of ligand tilt and that the steric bulk at the E11 position may be responsible for the extent of ligand tilt.

For the E11 Ala single point mutant V[E11]A, reduced steric bulk leads to only approximately one-half the tilt magnitude (β = 8.5°) compared to that in WT (β = 16.0), consistent with our proposal that the extent of tilt is determined primarily by the E11 rather than the E7 side-chain bulk. The direction of tilt is rotated toward the β-meso-H as compared to WT, but the magnitude of the apparent rotation, $\sim$20°, is within the uncertainty of each determination ($\sim$10°). The apparent change in the direction of the tilt, however, is also consistent with the expectations based on the reduced steric bulk of the E11 residue. On the other hand, both the extent (β = 15.5°) and direction (α = 4°) of tilt for V[E11]I are changed insignificantly from those in WT (Table 2). The failure of the V[E11]I mutant to exhibit increased ligand tilt, in spite of the increased bulk of the substituted residue, can be attributed to the fact that the Ile is oriented such that the increased bulk (*i.e.*, $C_\delta H_3$) is oriented well away from the iron or ligand (Figure 5A).

Inspection of the Euler angles for the double mutants shows that the effects of the steric bulk at the E7 and E11 positions are largely additive. Thus, in the case of the H,V[E7,E11]G,A mutant, the ligand tilt, $\beta \sim 8°$, is the same as in the V[E11]A mutant ($\beta \sim 8.5°$), and the tilt is in the direction toward γ-meso-H ($\alpha \sim -38°$), the same as in the H[E7]G mutant ($\alpha \sim -35°$). Similarly, in the case of the H,V[E7,E11]G,I mutant, the ligand tilt, $\beta \sim 17°$, is similar to that in the V[E11]I mutant ($\beta \sim 15.5°$) and is tilted in the same direction ($\alpha \sim -43°$) as in the H[E7]G mutant ($\alpha \sim -35°$). The slightly larger extent of the tilt in the double mutant can be attributed to the fact that the ethyl group of the Ile is pointed toward the ligand (Figure 5B), whereas in the single mutant it is pointed away from the ligand (Figure 5A).

The present ^{1}H NMR data on ligand orientation clearly show that the residues at positions E7 and E11 modulate the extent and direction of tilt, which can be correlated with their steric bulk and disposition relative to the binding site. It is also of considerable interest that even in the H,V[E7,E11]G,A mutant, where the steric contributions to the ligand tilt from both the E7 and E11 residues are expected to be minimal, there is still an appreciable tilt ($\beta \sim 8°$). This is larger than what is seen for the CO tilt in human Hb crystal structures ($\beta \sim 6°$) (Derewanda *et al.*, 1990), which have the same distal residues as Mb. This suggests that, in addition to distal E7 and E11 residues, other factors must play a role in modulating ligand tilt.

Distal Structural Perturbations. The NOESY cross-peak pattern and the quality of the fits for the magnetic axis determinations support an essentially unperturbed proximal side of the heme. However, both NOE and relaxation data indicate minor structural changes for the conserved distal residues. A detailed analysis of the ratio of steady-state NOEs between heme and the E helix backbone, as well as E helix backbone dipolar shifts for H[E7]V metMbCN (Rajarathnam *et al.*, 1993), had shown that increases in Q(E11 $C_\alpha H$) = 3 and Q(E14 $C_\beta H_3$) = 0.71 (from 0.8 and 0.52, respectively, in WT) indicate a $\sim$0.5–0.8-Å movement of the E helix toward the iron. The smaller increases for Q(E11 $C_\alpha H$) in the range 1.8–2.2 and for Q(E11 $C_\beta H_3$) in the range $\sim$0.7 indicate somewhat smaller movements in the same general direction for the Gly64(E7) mutants, H[E7]G and H,V[E7,E11]G,I. For both of these E7 Gly mutants, the movement of the E helix appears likely to fill the void due to the loss of the bulky E7 imidazole side chain, as discussed previously (Rajarathnam *et al.*, 1993). The preliminary X-ray structure for H[E7]G MbCO reveals a small lateral movement of the E helix (G. N. Phillips, Jr., personal communication). For the V[E11]I mutant, the NOE ratios Q(E11 $C_\alpha H$) = 0.52 and Q(E14 $C_\beta H_3$) = 0.46 are only marginally different from those in WT, indicating that the E helix has not moved significantly laterally. However, the increase in the E11 $C_\alpha H$ T_1 from 110 ± 15 ms in WT to 143 ± 20 ms in V[E11]I metMbCN suggests that the E helix might have moved slightly farther (0.1–0.2 Å) from the iron. Lastly, the NOE ratios for V[E11]A, Q(E11 $C_\alpha H$) = 0.29 and Q(E14 $C_\beta H_3$) = 0.46, are smaller than in WT, indicating that the E helix has moved away from the iron slightly.

The clear perturbation of the E helix in the distal pocket is one of the major reasons that the magnetic axes determined from the proximal side do not allow a more quantitative description of the Ile68(E11) orientation by their dipolar shifts. The quantitative estimation of the movement of the E helix in the present mutants requires more assignments and NOE constraints than are presently available and is therefore not pursued. This is in contrast to H[E7]V metMbCN, where the orientation of the substituted Val64(E7) could be determined from a combination of NOEs to the other side-chain protons and the heme (Rajarathnam *et al.*, 1993). While the apparent movement of the E helix in these mutants does not negate our conclusion that the magnitude of ligand tilt is determined by the E11 residue bulk and the direction of tilt

is determined by the E7 residue bulk, it does indicate that caution should be exercised in the detail to which the distal interactions are interpreted in terms of the WT structure. Moreover, since it is not only the ligand tilt magnitude/direction that respond to E7/E11 mutation but also the position of the whole E helix, it is clear that the tilting of the ligand cannot reliably measure the energetics of the distal steric interaction with the bound ligand.

Relationship of Tilt to Ligand Binding. Although the extent and direction of ligand tilt in metMbCN and MbCO are essentially the same in the WT (Kuriyan *et al.*, 1986; Emerson & La Mar, 1990b), the relative orientations are not known in the various mutants. However, it is likely that the response to distal steric influence on the FeCO unit will be very similar to that observed herein for the FeCN unit. Polarized infrared studies have shown that the ligand tilt in MbCO is not diminished in H[E7]G MbCO (Braunstein *et al.*, 1990). Preliminary X-ray data of the H[E7]G MbCO (G. N. Phillips, Jr., personal communication) mutant also indicate conserved tilt magnitude, with a small alteration in the direction of tilt in the same direction observed here for metMbCN by NMR. This raises the question of whether there is any real correlation between the extent of tilt and the kinetics of ligand binding.

V[E11]A Mb exhibits a higher CO binding constant by a factor ~2.5 and V[E11]I Mb displays a lower CO binding constant by a factor ~5 compared to WT, with the differences originating largely in altered on-rates (Egeberg *et al.*, 1990). While the on-rates correlate with steric bulk, faster for reduced (Ala) and slower for increased steric bulk (Ile), the very similar tilt in V[E11]I and WT metMbCN is inconsistent with any simple correlation between ligation rate and ligand tilt. The absence of such a correlation becomes more apparent when comparing a ~40-fold increase in CO affinity via an increased on-rate in H,V[E7,E11]G,A relative to V[E11]A (Egeberg *et al.*, 1990), even though both mutants exhibit essentially the same tilt angle (~8–9°). The clear absence of a correlation between steric ligand tilt and ligation dynamics and thermodynamics suggests that other properties, such as heme pocket polarity, modulate CO ligation in these mutants.

CONCLUSIONS

The dipolar contacts among the amino acids and heme on the proximal side dictate a highly conserved structure with respect to WT Mb, and the significantly altered dipolar shifts for these proximal protons allow the quantitative determination of the orientation of the magnetic axes of the susceptibility tensor. On the basis of the orientation of the major magnetic axes serving as a direct indication of ligand tilt, it is concluded that the steric bulk of the residue at position E11 plays a key role in determining the extent of tilt of the ligand from the heme normal, while the steric bulk of the residue at position E7 plays a key role in controlling the direction of the ligand tilt on the heme plane. Simultaneous mutations at positions E7 and E11 produce additive effects on ligand tilt/direction. The absence of any correlation between the degree of ligand tilt and the rates of ligation in these mutants dictates that factors other than steric bulk, such as heme pocket polarity, play an important role in modulating ligand binding.

ACKNOWLEDGMENT

The authors are indebted to K. Vyas for assistance with data processing and to G. N. Phillips for providing the X-ray coordinates for H[E7]G MbCO.

SUPPLEMENTARY MATERIAL AVAILABLE

Six tables (heme chemical shifts for mutant metMbCN, effect of input data on Euler angles, and observed *vs* calculated dipolar shifts for four mutants) and four figures (COSY and the steady-state NOEs for V[E11]A metMbCN; COSY and NOESY data for V[E11]I metMbCN) (10 pages). Information for obtaining this data is provided on any current masthead page.

REFERENCES

Aue, W. P., Bartholdi, E., & Ernst, R. R. (1976) *J. Chem. Phys. 64*, 2229–2246.
Balasubramanian, S., Lambright, D. G., Marden, M. C., & Boxer, S. G. (1993) *Biochemistry 32*, 2202–2212.
Bolognesi, M., Onesti, S., Gatti, G., Coda, A., Ascenzi, P., Giacometti, A., & Brunori, M. (1989) *J. Mol. Biol. 205*, 529–544.
Bolognesi, M., Coda, A., Frigerio, F., Gatti, G., Ascenzi, P., & Brunori, M. (1990) *J. Mol. Biol. 225*, 621–625.
Braunstein, D., Ansari, A., Berendzen, J., Cowen, B. R., Egeberg, K. D., Frauenfelder, H., Hong, M. K., Ormos, P., Sauke, T. B., Scholl, R., Schulte, A., Sligar, S. G., Springer, B. A., Steinbach, P. J., & Young, R. D. (1988) *Proc. Natl. Acad. Sci. U.S.A. 85*, 8497–8501.
Carver, T. E., Brantley, R. E., Singleton, E. W., Arduini, R. M., Quillin, M. L., Phillips, G. N., & Olson, J. S. (1992) *J. Biol. Chem. 267*, 14443–14450.
Case, D. A., & Karplus, M. (1979) *J. Mol. Biol. 123*, 343–368.
Cheng, X., & Schoenborn, B. P. (1991) *J. Mol. Biol. 220*, 381–399.
Chiu, M. (1992) Ph.D. Dissertation, University of Illinois, Urbana–Champaign, IL.
Collman, J. P., Brauman, J. I., Halbert, T. R., & Suslick, K. (1976) *Proc. Natl. Acad. Sci. U.S.A. 73*, 3333–3337.
Conti, E., Moser, C., Rizzi, M., Mattevi, A., Lionetti, C., Coda, A., Ascenzi, P., & Bolognesi, M. (1993) *J. Mol. Biol. 233*, 498–508.
Cross, K. J., & Wright, P. E. (1985) *J. Magn. Reson. 64*, 220–231.
Dalvit, C., & Wright, P. E. (1987) *J. Mol. Biol. 194*, 313–327.
Deatherage, J. F., Loe, R. S., Anderson, C. M., & Moffat, K. (1976) *J. Mol. Biol. 104*, 687–706.
Derewenda, Z., Dodson, G., Emsley, P., Harris, D., Nagai, K., Perutz, M., & Renaud, J.-P. (1990) *J. Mol. Biol. 211*, 515–519.
Dickerson, R. E., & Geis, I. (1983) *Hemoglobin: Structure, Function, Evolution and Pathology* (Hagopian, P., Ed.) Benjamin/Cummings, Menlo Park, CA.
Egeberg, K. D., Springer, B. A., Sligar, S. G., Carver, T. E., Rohlfs, R. J., & Olson, J. S. (1990) *J. Biol. Chem. 265*, 11788–11795.
Elber, R., & Karplus, M. (1987) *Science 235*, 318–321.
Emerson, S. D., & La Mar, G. N. (1990a) *Biochemistry 29*, 1545–1556.
Emerson, S. D., & La Mar, G. N. (1990b) *Biochemistry 29*, 1556–1566.
Feng, Y., Roder, H., & Englander, S. W. (1990) *Biochemistry 29*, 3494–3504.
Gupta, R. K. (1976) *J. Magn. Reson. 24*, 461–465.
Jeener, J., Meier, B. H., Bachmann, P., & Ernst, R. R. (1979) *J. Chem. Phys. 71*, 4546–4553.
Kottalam, J., & Case, D. A. (1988) *J. Am. Chem. Soc. 110*, 7690–7697.
Kuriyan, J., Wilz, S., Karplus, M., & Petsko, G. A. (1986) *J. Mol. Biol. 192*, 133–154.
Mattevi, A., Gatti, G., Coda, A., Rizzi, M., Ascenzi, P., Brunori, M., & Bolognesi, M. (1991) *J. Mol. Recognit. 4*, 1–6.
Phillips, S. E. V. (1980) *J. Mol. Biol. 142*, 531–554.
Qin, J., La Mar, G. N., Ascoli, F., & Brunori, M. (1993a) *J. Mol. Biol. 231*, 1009–1023.

Qin, J., La Mar, G. N., Cutruzzolá, F., Travaglini Allocatelli, C., Branaccio, A., & Brunori, M. (1993b) *Biophys. J. 65*, 2178–2190.
Rajarathnam, K., La Mar, G. N., Chiu, M. L., & Sligar, S. G. (1992) *J. Am. Chem. Soc. 114*, 9048–9058.
Rajarathnam, K., Qin, J., La Mar, G. N., Chiu, M. L., & Sligar, S. G. (1993) *Biochemistry 32*, 5670–5680.
Rohlfs, R. J., Mathews, A. J., Carver, T. E., Olson, J. S., Springer, B. A., Egeberg, K. D., & Sligar, S. G. (1990) *J. Biol. Chem. 265*, 3168–3176.
Shulman, R. G., Glarum, S. H., & Karplus, M. (1971) *J. Mol. Biol. 57*, 93–115.
Smerdon, S. J., Dodson, G. G., Wilkinson, A. J., Gibson, Q. H., Blackmore, R. S., Carver, T. E., & Olson, J. S. (1991) *Biochemistry 30*, 6252–6260.
Springer, B. A., & Sligar, S. G. (1987) *Proc. Natl. Acad. Sci. U.S.A. 84*, 8961–8965.
States, D. J., Haberkorn, R. A., & Ruben, D. J. (1982) *J. Magn. Reson. 48*, 286–292.
Steigemann, W., & Weber, E. (1979) *J. Mol. Biol. 127*, 309–338.
Theriault, Y., Pochapsky, T. C., Dalvit, C., Chiu, M. L., Sligar, S. G., & Wright, P. E. (1994) *J. Biomol. Nucl. Magn. Reson.* (in press).
Wishart, D. S., Sykes, B. D., & Richards, F. M. (1991) *J. Mol. Biol. 222*, 311–333.
Yu, L. P., La Mar, G. N., & Rajarathnam, K. (1990) *J. Am. Chem. Soc. 112*, 9527–9534.